

OPEN ACCESS

Comparative Study of Indium as a Filler or as a Substitute in Yb-Filled Ni-Doped CoSb_3

To cite this article: Keshav Prasad Dabral *et al* 2023 *ECS Adv.* **2** 044001

View the [article online](#) for updates and enhancements.

You may also like

- [Advanced functional magnetic microwires for technological applications](#)
Arcady Zhukov, Paula Corte-Leon, Lorena Gonzalez-Legarreta et al.
- [Regulating phase change behavior and surface characteristics of \$\text{Sn}_{1-x}\text{Sb}_x\$ thin film by oxygen doping](#)
Yifeng Hu, Haipeng You, Qingqian Chou et al.
- [Thermoelectric power factor of ternary single-crystalline \$\text{Sb}_2\text{Te}_3\$ - and \$\text{Bi}_2\text{Te}_3\$ -based nanowires](#)
Svenja Bäßler, Tim Böhnert, Johannes Gooth et al.



245th ECS Meeting • May 26-30, 2024 • San Francisco, CA

Don't miss your chance to present!

Connect with the leading electrochemical and solid-state science network!

Deadline Extended: December 15, 2023

Submit now!





Comparative Study of Indium as a Filler or as a Substitute in Yb-Filled Ni-Doped CoSb₃

Keshav Prasad Dabral,^{1,z} Kalpna Rajput,² Krishna Dabral,³ and Ajay Singh Verma⁴

¹Department of Physics, School of Allied Science, Dev Bhoomi Uttarakhand University, Navgaon, Manduwala, Dehradun 248007, Uttarakhand, India

²Indian Institute of Technology Bombay, Powai, Mumbai 400076, India

³Rajkiya Mahavidhyalaya Chinyalisaur, Uttarkashi, Uttarakhand 249196 India

⁴Division of Research and Innovation Uttarakhand University Dehradun 248007 India

CoSb₃ with an open structure that can accommodate several fillers has been extensively studied due to its PGEC character. It is known that partial substitution of Ni with Co generates more free electron and alter the CoSb₃ into a stable n-type skutterudite. In this work, we used In as a filler with Yb and as a partial substitution of Sb in Co_{3.85}Ni_{0.15}Sb₁₂. All alloys have been synthesized by solid-state reaction method and hot press processes. The Seebeck coefficient varies from 160 μ VK⁻¹ to 200 μ VK⁻¹ in Yb_{0.3}Co_{3.85}Ni_{0.15}Sb_{11.5}In_{0.5}, however, it exhibits the highest charge carrier concentration. Yb_{0.3}Co_{3.85}Ni_{0.15}Sb_{11.5}In_{0.5} exhibits the highest power factor of 3.9 mW⁻¹K⁻² at 723 K, which is 20% and 15% larger than a single-filled and double-filled Ni-doped system respectively. The suitable amount of In doped with Sb in a Ni-doped single-filled skutterudite system resulted is not only an improvement of the thermopower but also a decrease of the thermal conductivity due to enhanced point-defect scattering and increased electron-phonon interaction. Hence Yb_{0.3}Co_{3.85}Ni_{0.15}Sb_{11.5}In_{0.5} exhibits a maximum zT of 1.25 which is 25% higher than Yb_{0.2}In_{0.2}.Co_{3.85}Ni_{0.5}Sb₁₂. Therefore, indium is also a good option to use as a substitution, n-type skutterudite compared to use as a filler.

© 2023 The Author(s). Published on behalf of The Electrochemical Society by IOP Publishing Limited. This is an open access article distributed under the terms of the Creative Commons Attribution 4.0 License (CC BY, <http://creativecommons.org/licenses/by/4.0/>), which permits unrestricted reuse of the work in any medium, provided the original work is properly cited. [DOI: 10.1149/2754-2734/ad10e2]



Manuscript submitted April 27, 2023; revised manuscript received September 22, 2023. Published December 7, 2023.

Thermoelectric (TE) technology is an important part of clean, eco-friendly, renewable energy for a sustainable future in terms of waste heat conversion into electricity. The performance of any TE material depends on the figure of merit

$$zT = \frac{S^2\sigma}{\kappa}T, \quad [1]$$

where S is the Seebeck coefficient, σ is electrical conductivity, κ is total thermal conductivity that includes electronic (κ_e) and lattice (κ_l) part and T is the average absolute temperature, respectively.

Several compounds have been investigated for thermoelectric application, for example, half Huesler alloys, oxides, chalcogenides, clathrates, skutterudites, etc. Among these, binary skutterudites are suitable for medium-temperature applications as filling the voids in these structures will form a material with low thermal conductivity similar to that of glass and good electrical properties identical to those of a crystal.^{1,2} The binary skutterudite compounds have the general chemical formula MX₃, where M is typically one of the column 9 transition metals (Co, Rh, or Ir), and X is one of the elements P, As, or Sb (often called pincogen). The skutterudites have a cubic crystal structure belonging to the space group *Im* $\bar{3}$ (204).³ A high thermal conductivity causes the binary skutterudite compounds to have a low figure of merit. However, the skutterudites' crystal structure provides an opportunity to reduce thermal conductivity. It has two large voids in each unit cell, which can be filled by inserting various guest atoms, such as rare Earth, alkaline Earth, and alkali metals, into these voids. The guest atoms are loosely bound with the host atoms, so the "rattling" of these guest atoms effectively scatters phonons and reduces the lattice's thermal conductivity without significantly degrading the electrical properties.⁴⁻¹² Yb has been extensively used compared to other materials as filled due to its high filling fraction in the voids.¹³⁻¹⁶

In containing CoSb₃ based skutterudite have attracted much attention due to the high thermoelectric efficiency and mid temperature range application in automotive waste heat recovery. However there has been much debate over how much indium is actually

suitable in CoSb₃ or it simply precipitates out as nano particles. Highest zT was reported 1.2 for In_{0.25}Co₄Sb₁₂ at 575 K by He et al.¹⁷ in the single filling, zT of 1.43 for In_{0.2}Ce_{0.15}Co₄Sb₁₂ at 800 K was reported by Li et al.¹⁸ in the double filling. However, the nature of In incorporation has not been fully understood and there are several different mechanisms for enhancement of zT. One possible mechanism is that the In atom goes into the filler site and due to the rattling and avoided crossing effect,¹⁹ the thermal conductivity gradually decreased, which enhanced zT; another possible mechanism is that doping of In results in a nanostructured InSb phase that is evenly distributed on the boundaries of the skutterudite phase, which reduced thermal conductivity and enhanced zT.²⁰ So, which mechanism accounts for the good thermoelectric properties of In-doping skutterudites remains unclear. There has been much debate about the solubility limit x, of indium in In_xCo₄Sb₁₂ which is found that due to the charge-compensated compound defects (CCD) In enters into the void filling.²¹

Partly substituting Co with Ni generates more free electrons and alters the CoSb₃ into a stable n-type skutterudite.²²⁻²⁵ In this work, we introduced Yb and In as fillers and studied their elevated temperature thermoelectric properties. We also partially substituted In with Sb in this Yb-filled Ni-doped system and studied indium role as a substitution in n-type skutterudites.

Experimental

All alloys have been synthesized from Co powder, Yb chunks, Ni powder, In chunks, and Sb beads all with 99.999% purity. The stoichiometric quantities of the element are weighted and loaded in a quartz ampule and sealed in an inert atmosphere of 10⁻⁴ Torr. The quartz tube was placed in a furnace, held at 1050 °C for 10 h, and quenched in water. The resulting ingot was powdered, cold pressed into a pellet and sealed in an evacuated quartz tube. The pellet was annealed for 100 h at 650 °C and subsequently hot-pressed at 600 °C under a pressure of 60 MPa for 12 min. The density of these pellets determined using the Archimedes' principle was >95%. The circular pellets were used to measure the thermal diffusivity in the laser flash system, Netzch LFA 457 while a parallelepiped cut from this pellet was used to measure the high-temperature electrical resistivity and Seebeck Coefficient. The thermal conductivity of the alloys was

^zE-mail: Keshav.dabral@gmail.com

Table I. The diffraction pattern fitting quality parameters R_p , R_{wp} and χ^2 of the alloys $\text{Yb}_{0.2}\text{In}_{0.2}\text{Co}_{3.85}\text{Ni}_{0.5}\text{Sb}_{12}$ and $\text{Yb}_{0.3}\text{Co}_{3.85}\text{Ni}_{0.15}\text{Sb}_{11.5}\text{In}_{0.5}$ given in the table.

Sample	R_p	R_{wp}	χ^2
$\text{Yb}_{0.2}\text{In}_{0.2}\text{Co}_{3.85}\text{Ni}_{0.5}\text{Sb}_{12}$	19	10.8	3.9
$\text{Yb}_{0.3}\text{Co}_{3.85}\text{Ni}_{0.15}\text{Sb}_{11.5}\text{In}_{0.5}$	20	12.7	5.1

calculated using the measured thermal diffusivity, heat capacity and density. The microstructural investigation of the alloys was performed using a combination of X-ray diffraction (Cu- $K\alpha_1$ radiation obtained from a 9 kW rotating anode source Rigaku 9 kW). The room temperature transport parameters, Hall mobility and carrier concentration, were determined using van der Pauw sample geometry in a field of 1 T.

Results and Discussion

The XRD pattern of all three alloys (indium filled, indium substituted, without indium) along their Rietveld refinement analysis is shown in Figs. 1 and 2 and the diffraction pattern fitting quality parameters R_p , R_{wp} and χ^2 of the alloys shown in Table I. The inset of Fig. 1 shows that the peak is shifting to the left side, and the lattice constant increased from 0.9034 nm to 0.9056 nm due to Sb ring deformation in partial substitution of Sb with In. Both alloys show the presence of the single-phase skutterudite with minute secondary phases of InSb and Sb. It is observed that In not entering entirely as a filler in, $\text{Yb}_{0.2}\text{In}_{0.2}\text{Co}_{3.85}\text{Ni}_{0.5}\text{Sb}_{12}$ which was also shown in $\text{In}_x\text{Yb}_y\text{Co}_4\text{Sb}_{12}$ with a solubility limit of In is less than 0.20²⁶ and in $\text{In}_x\text{Ce}_y\text{Co}_4\text{Sb}_{12}$ with 0.15.¹⁸

It is found that with an indium addition of $x = 0.3$ in $\text{In}_x\text{Co}_4\text{Sb}_{12}$, Sb was found at the grain boundaries of the skutterudite phase, which suggests that partial substitution of Sb adds complexity to the possible position that the In atom may go to voids. Such a substitution was also deduced in the related $\text{Ga}_x\text{Co}_4\text{Sb}_{12-x/3}$ where Ga, like In, is a group 13 element in the periodic table. It is known that one In atom at the Sb 24 g site generates a deficiency of two electrons and one In atom at the void-filling 2a position adds one extra electron compared to pure CoSb_3 . Therefore we can say that the In atom goes to the filler site and Sb site at the same time and the solubility of indium in the skutterudite phase is reduced to $x = 0.09$ when it coexists in equilibrium with InSb and Sb²⁷ due to charge-compensated compound defects (CCD).²¹

Figure 3a shows the temperature dependent of the electrical conductivity of all alloys. The electrical conductivity of all alloys is nearly constant and does not change with increasing temperature. However, $\text{Yb}_{0.3}\text{Co}_{3.85}\text{Ni}_{0.15}\text{Sb}_{11.5}\text{In}_{0.5}$ exhibits the highest σ of $12 \times 10^4 \text{ S m}^{-1}$, confirming that indium acts as a n-type dopant to increase the charge carrier concentration. The electrical conductivity of the Ni-doped system increases after inserting Yb and In as filler due to an increase in charge carrier concentration shown in Table II. $\text{Yb}_{0.2}\text{Co}_{3.85}\text{Ni}_{0.15}\text{Sb}_{11.5}\text{In}_{0.5}$ exhibits the lowest mobility μ_H of $11 \text{ cm}^2\text{V}^{-1}\text{s}^{-1}$ due to electron-electron scattering, which takes place from the partial substitution of In and Ni. Intrinsic CoSb_3 is a valence-precise semiconductor where the doping effect of defects can be understood with Zintl chemistry. Here an indium atom at the void filling site (In_{VF}) shows an effective charge state +1 and contributes one extra electron to the doped system. Indium atoms at the Sb-substitutional site accept two electrons. Thus, $\text{Yb}_{0.3}\text{Co}_{3.85}\text{Ni}_{0.15}\text{Sb}_{11.5}\text{In}_{0.5}$ should also be a valence-precise semiconductor. The relatively high electron concentrations (as measured by Hall effect) of $\text{Yb}_{0.3}\text{Co}_{3.85}\text{Ni}_{0.15}\text{Sb}_{11.5}\text{In}_{0.5}$ compared to, $\text{Yb}_{0.2}\text{In}_{0.2}\text{Co}_{3.85}\text{Ni}_{0.5}\text{Sb}_{12}$ suggests that the indium defects are not entirely charge compensated, with some excess indium as electron donor defects most likely In_{VF} also present.²⁸

The temperature dependent Seebeck coefficient of all alloys are illustrated in Fig. 3b. The Seebeck coefficient of alloys increased

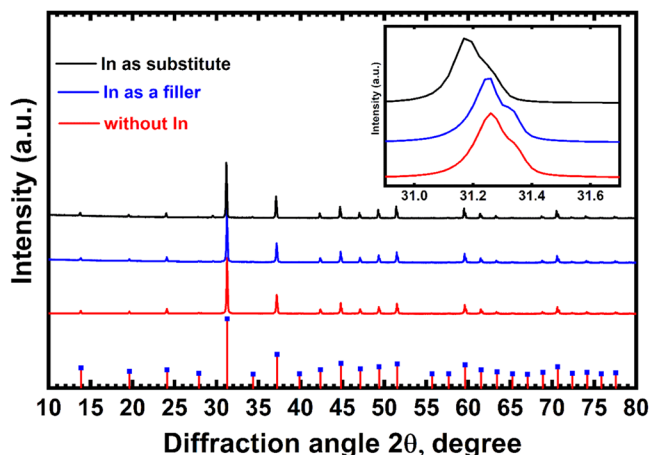


Figure 1. XRD pattern of the alloys $\text{Yb}_{0.3}\text{Co}_{3.85}\text{Ni}_{0.5}\text{Sb}_{12}$, $\text{Yb}_{0.2}\text{In}_{0.2}\text{Co}_{3.85}\text{Ni}_{0.5}\text{Sb}_{12}$, $\text{Yb}_{0.3}\text{Co}_{3.85}\text{Ni}_{0.15}\text{Sb}_{11.5}\text{In}_{0.5}$.

with increasing temperature up to 700 K after which a decrease was observed due to bipolar conduction. Seebeck coefficient also decreased after inserting Yb and In as a filler, which generates more free electrons to the system. The Seebeck coefficient varies from $160 \mu\text{VK}^{-1}$ to $200 \mu\text{VK}^{-1}$ in $\text{Yb}_{0.3}\text{Co}_{3.85}\text{Ni}_{0.15}\text{Sb}_{11.5}\text{In}_{0.5}$; however, it shows the highest charge carrier concentration. It was due to the unique band structure, with a valence band formed by the orbital hybridization among the particular 4 f states of the fillers, 3d states of the transition metals, and 5p states of the pnictides as well as to the enhancement of effective mass due to the narrow 4 f band effects of rare Earth metal.^{29,30}

Figure 4a represents the temperature dependence of the thermal conductivity of all specimens. The thermal conductivity of all alloys decreased with increasing temperatures up to 700 K, after which an increase was observed due to bipolar diffusion at high temperatures. Thermal conductivity of $\text{Co}_{3.85}\text{Ni}_{0.15}\text{Sb}_{12}$ reduced to half after filling of Yb and In in the voids. $\text{Yb}_{0.3}\text{Co}_{3.85}\text{Ni}_{0.15}\text{Sb}_{11.5}\text{In}_{0.5}$ exhibits the lowest thermal conductivity of $\sim 2.5 \text{ Wm}^{-1}\text{K}^{-1}$ through all temperatures among all. The contribution of charge carriers to κ in both sets of alloys has been estimated using the Wiedemann–Franz relation and determining the Lorentz factor as a function of T using the statistical relation.³¹ The Lorentz number in all the different alloys determined using this SPB model is found to decrease with T from a typically degenerate value to a nondegenerate value, shown in the inset of Fig. 4b.

The reduction of lattice thermal conductivity in $\text{Yb}_{0.3}\text{Co}_{3.85}\text{Ni}_{0.15}\text{Sb}_{11.5}$ could be explained by the dual-site occupation of indium impurities with complex compound defect and, a dual-character phonon scattering mechanism. The indium impurity at the Sb-substitutional site establishes a point defect with size and bonding (in addition to slight mass) mismatch from the host Sb atoms, leading to the scattering of high-frequency lattice phonons. The indium atoms at the void sites behave as a typical filler species and scatter long wavelength phonons via resonant scattering and avoided crossing mechanisms. Therefore, the effective reduction of κ_L implies that a broad spectrum of lattice phonons could be scattered in the In-containing skutterudites with a complex compound defect. The relatively high indium doping content at both the void and Sb sites, is important as it controls the magnitude of the phonon scattering effect.^{32,33}

The temperature dependence of the power factor for the different alloys has been determined using the measured electrical conductivity and Seebeck coefficient by the equation power factor = $s^2\sigma$ and is shown in Fig. 5a. $\text{Yb}_{0.3}\text{Co}_{3.85}\text{Ni}_{0.15}\text{Sb}_{11.5}\text{In}_{0.5}$ sample exhibits the highest power factor of $3.9 \text{ mW}^{-1}\text{K}^{-2}$ at 723 K among all alloys, 15% larger than In filled Ni-doped system respectively. Dimensionless figure-of-merit zT was calculated by the power factor and thermal conductivity shown in Fig. 5b. $\text{Yb}_{0.3}\text{Co}_{3.85}\text{Ni}_{0.15}\text{Sb}_{11.5}\text{In}_{0.5}$ exhibits

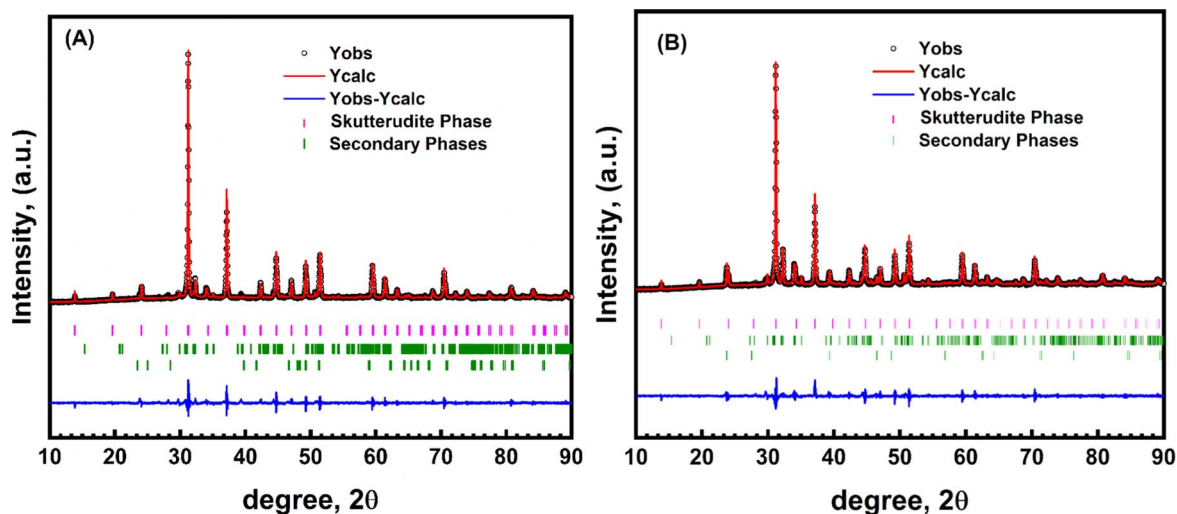


Figure 2. The powder diffraction patterns obtained using Cu-K α radiation have been analysed using Rietveld refinement of the phases and structure. The refined diffraction patterns together with experimental data is shown for (A) $\text{Yb}_{0.3}\text{Co}_{3.85}\text{Ni}_{0.15}\text{Sb}_{11.5}\text{In}_{0.5}$ (B) $\text{Yb}_{0.2}\text{In}_{0.2}\text{Co}_{3.85}\text{Ni}_{0.5}\text{Sb}_{12}$.

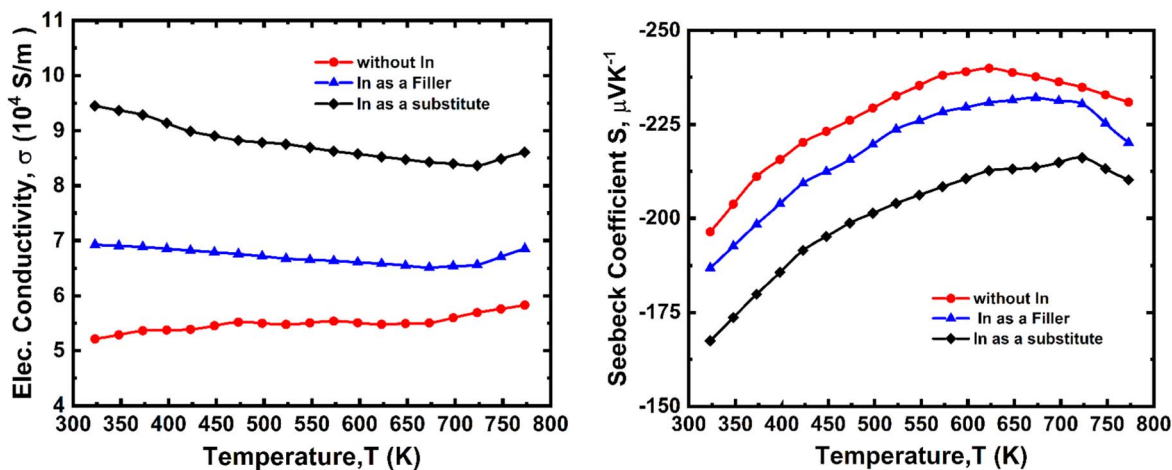


Figure 3. Temperature-dependent (a) electrical conductivity (b) Seebeck Coefficient of the alloys the $\text{Yb}_{0.3}\text{Co}_{3.85}\text{Ni}_{0.5}\text{Sb}_{12}$, $\text{Yb}_{0.2}\text{In}_{0.2}\text{Co}_{3.85}\text{Ni}_{0.5}\text{Sb}_{12}$, and $\text{Yb}_{0.3}\text{Co}_{3.85}\text{Ni}_{0.15}\text{Sb}_{11.5}\text{In}_{0.5}$.

Table II. Room temperature transport properties along with their lattice constant for all alloys.

Sample	a (nm)	Relative Density	n (10^{20} cm^{-3})	μ ($\text{cm}^2 \text{ V}^{-1} \text{ s}^{-1}$)	σ (Sm^{-1})	S (μVK^{-1})	K ($\text{Wm}^{-1}\text{K}^{-1}$)
$\text{Co}_{3.85}\text{Ni}_{0.15}\text{Sb}_{12}$	0.9034	97%	0.85	21	29132	240	5.7
$\text{Yb}_{0.3}\text{Co}_{3.85}\text{Ni}_{0.5}\text{Sb}_{12}$	0.9046	97%	1.2	22	52126	196	3.2
$\text{Yb}_{0.2}\text{In}_{0.2}\text{Co}_{3.85}\text{Ni}_{0.5}\text{Sb}_{12}$	0.9051	97%	2.9	27	69260	186	3.1
$\text{Yb}_{0.3}\text{Co}_{3.85}\text{Ni}_{0.15}\text{Sb}_{11.5}\text{In}_{0.5}$	0.9056	96%	5.6	11	94508	167	2.4

maximum zT of 1.25 at 723 K which is 25% higher than $\text{Yb}_{0.2}\text{In}_{0.2}\text{Co}_{3.85}\text{Ni}_{0.5}\text{Sb}_{12}$.

Conclusions

All alloys have been synthesized by solid-state reaction method and hot press processes. The XRD result and Reitveld refinement indicated that a single doped skutterudite phase was obtained with minute secondary phases. It is found that partial substitution of Co with Ni and Sb with In has a synergic beneficial effect on the skutterudite system. The appropriate amount of In in Ni-doped

single-filled skutterudite system resulted in not only an improvement of the thermopower but also a decrease of the thermal conductivity due to enhanced point-defect scattering and increased electron-phonon interaction. $\text{Yb}_{0.3}\text{Co}_{3.85}\text{Ni}_{0.15}\text{Sb}_{11.5}\text{In}_{0.5}$ showed the highest zT of 1.25 at 723 K, which is 40% higher than double filled, $\text{Yb}_{0.2}\text{In}_{0.2}\text{Co}_{3.85}\text{Ni}_{0.5}\text{Sb}_{12}$. Therefore In is an excellent option to use as a dopant in single-filled n-type skutterudite compared to a filler. The relatively more significant carrier concentrations compared to In filled skutterudites indicate the possibility of not fully charge-compensated compound defects, which means that single-filling defects may coexist with dual-site compound defects. Better

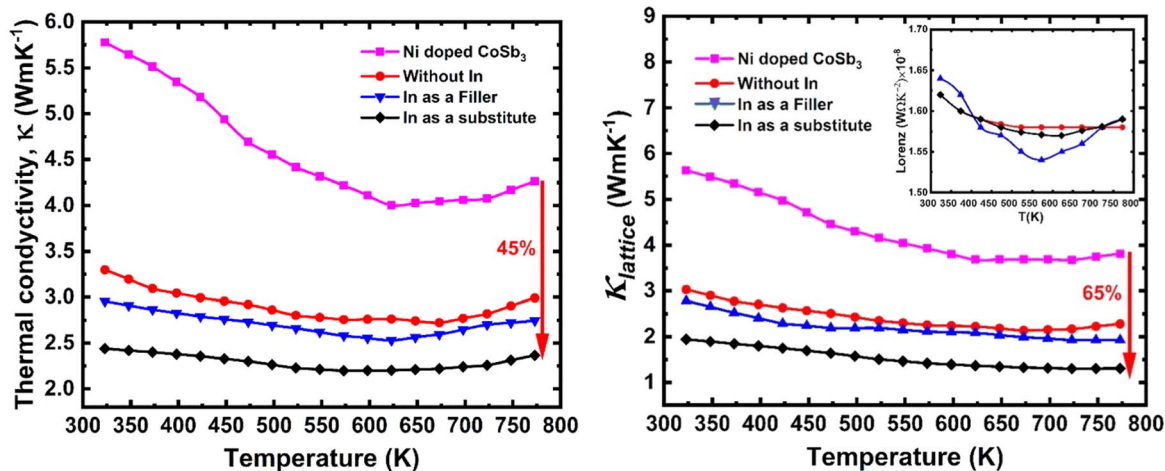


Figure 4. Temperature dependent (a) Thermal Conductivity (b) Lattice Thermal conductivity of the alloys the $\text{Yb}_{0.3}\text{Co}_{3.85}\text{Ni}_{0.5}\text{Sb}_{12}$, $\text{Yb}_{0.2}\text{In}_{0.2}\text{Co}_{3.85}\text{Ni}_{0.5}\text{Sb}_{12}$, $\text{Yb}_{0.3}\text{Co}_{3.85}\text{Ni}_{0.15}\text{Sb}_{11.5}\text{In}_{0.5}$. Calculated Lorenz numbers are shown in the inset of Fig. 4b.

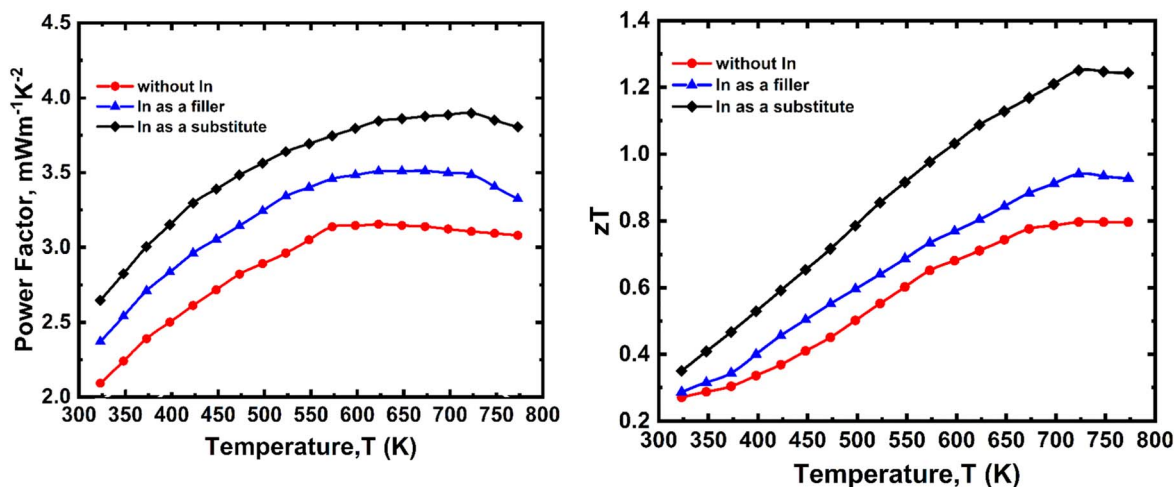


Figure 5. Temperature dependent of (a) Power factor (b) figure-of-merit of alloys $\text{Yb}_{0.3}\text{Co}_{3.85}\text{Ni}_{0.5}\text{Sb}_{12}$, $\text{Yb}_{0.2}\text{In}_{0.2}\text{Co}_{3.85}\text{Ni}_{0.5}\text{Sb}_{12}$, $\text{Yb}_{0.3}\text{Co}_{3.85}\text{Ni}_{0.15}\text{Sb}_{11.5}\text{In}_{0.5}$.

performance of this alloy could be achieved by optimizing the proportion of Ni, In, and exploring other fillers instead of Yb, which results in a significant power factor. On the other hand, compared to In as filler, substituted In effectively decreased lattice thermal conductivity due to alloy scattering.

Acknowledgments

The authors wish to thank DST, IITB-ISRO space technology cell, BRNS and IITB for assistance at various stages. The authors also want to acknowledge the Inspire fellowship program of DST.

ORCID

Keshav Prasad Dabral  <https://orcid.org/0000-0001-7499-4093>

References

- G. Rogl and P. Rogl, "Skutterudites, a most promising group of thermoelectric materials." *Current Opinion in Green and Sustainable Chemistry*, **4**, 50 (2017).
- M. Rull-Bravo et al., "Skutterudites as thermoelectric materials: revisited." *RSC Adv.*, **5**, 41653 (2015).
- G. S. Nolas, D. T. Morelli, and T. M. Tritt, "SKUTTERUDITES: a phonon-glass-electron crystal approach to advanced thermoelectric energy conversion applications." *Annu. Rev. Mater. Sci.*, **29**, 89 (1999).
- B. C. Sales et al., "Filled skutterudite antimonides: electron crystals and phonon glasses." *Physical Review B*, **56**, 15081 (1997).
- T. Caillat, J. P. Fleurial, and A. Borsichevsky, "Bridgman-solution crystal growth and characterization of the skutterudite compounds CoSb_3 and RhSb_3 ." *J. Cryst. Growth*, **166**, 722 (1996).
- D. T. Morelli et al., "Cerium filling and doping of cobalt triantimonide." *Physical Review B*, **56**, 7376 (1997).
- B. Ryll et al., "Structure, phase composition, and thermoelectric properties of $\text{YbCo}_4\text{Sb}_{12}$ and their dependence on synthesis method." *ACS Appl. Energy Mater.*, **1**, 113 (2018).
- Y. Li et al., "Enhanced thermoelectric performance in rare-earth filled-skutterudites." *J. Mater. Chem. C*, **4**, 4374 (2016).
- K.-H. Park et al., "Thermoelectric properties of Yb-filled CoSb_3 skutterudites." *J. Korean Phys. Soc.*, **65**, 491 (2014).
- W. Li and N. Mingo, "Thermal conductivity of fully filled skutterudites: role of the filler." *Phys. Rev.*, **B89**, 184304 (2014).
- K. P. Dabral and S. Vitta, "p-type high temperature thermoelectric behavior of dy filled CoSb_3 and $\text{Fe}_{1.5}\text{Co}_{2.5}\text{Sb}_{12}$ and their magnetic properties." *ACS Appl. Energy Mater.*, **3**, 6644 (2020).
- K. P. Dabral and S. Vitta, "Tuning the nature of charge carriers by controlling dual substitution in single-filled thermoelectric skutterudite, Yb- CoSb_3 ." *Emergent Materials*, **3**, 195 (2020).
- H. Li et al., "Preparation and thermoelectric properties of high-performance Sb additional $\text{Yb}_{0.2}\text{Co}_4\text{Sb}_{12+y}$ bulk materials with nanostructure." *Appl. Phys. Lett.*, **92**, 202114 (2008).
- H. Y. Geng, S. Ochi, and J. Q. Guo, "Solidification contraction-free synthesis for the $\text{Yb}_{0.15}\text{Co}_4\text{Sb}_{12}$ bulk material." *Appl. Phys. Lett.*, **91**, 022106 (2007).
- S. Wang et al., "High-performance n-type $\text{YbCo}_4\text{Sb}_{12}$: from partially filled skutterudites towards composite thermoelectrics." *NPG Asia Mater.*, **8**, e285 (2016).
- L. Fu et al., "enhancement of thermoelectric properties of Yb-filled skutterudites by an Ni-Induced 'core-shell' structure." *J. Mater. Chem. A*, **3**, 1010 (2015).
- T. He et al., "Thermoelectric properties of indium-filled skutterudites." *Chem. Mater.*, **18**, 759 (2006).
- H. Li et al., "High performance $\text{In}_x\text{Ce}_y\text{Co}_4\text{Sb}_{12}$ thermoelectric materials with in situ forming nanostructured InSb phase." *Appl. Phys. Lett.*, **94**, 102114 (2009).

19. M. Christensen et al., "Avoided crossing of rattler modes in thermoelectric materials." *Nat. Mater.*, **7**, 811 (2008).
20. K. P. Dabral and S. Vitta, "Effect of In As Sb substitute on thermoelectric properties of Yb filled CoSb₃ skutterudite." *AIP Conf. Proc.*, **2265**, 030444 (2020).
21. Y. Qiu et al., "Charge-compensated compound defects in ga-containing thermoelectric skutterudites." **23**, 3194 (2013).
22. L. Kong et al., "Influence of the high pressure and high temperature synthesis on thermoelectric properties of Ni-doped skutterudite." *J. Alloys Compd.*, **697**, 257 (2017).
23. M. Kim et al., "Electronic transport properties of Ni-doped CoSb₃ prepared by encapsulated induction melting." *25th International Conference on Thermoelectrics 2006* (2006).
24. V. Trivedi et al., "Microstructure and doping effect on the enhancement of the thermoelectric properties of Ni doped Dy filled CoSb₃ skutterudites." *Sustainable Energy & Fuels*, **2**, 2687 (2018).
25. L. Kong et al., "N-type Ba_{0.3}Ni_{0.15}Co_{3.85}Sb₁₂ skutterudite: high pressure processing technique and thermoelectric properties." *J. Alloys Compd.*, **734**, 36 (2018).
26. J. Graff et al., "High-Temperature thermoelectric properties of Co₄Sb₁₂-based skutterudites with multiple filler atoms: Ce_{0.1}In_xY_{by}Co₄Sb₁₂." *J. Electron. Mater.*, **40**, 696 (2011).
27. A. Grytsiv et al., "In_yCo₄Sb₁₂ skutterudite: phase equilibria and crystal structure." *J. Electron. Mater.*, **42**, 2940 (2013).
28. Y. Tang et al., "Phase diagram of In-Co-Sb system and thermoelectric properties of In-containing skutterudites." *Energy Environ. Sci.*, **7**, 812 (2014).
29. M. Puyet et al., "Influence of Ni on the thermoelectric properties of the partially filled calcium skutterudites Ca_yCo_{4-x}Ni_xSb₁₂." *Phys Rev B*, **75**, 245110 (2007).
30. G. Tan et al., "Enhanced thermoelectric performance in zinc substituted p-type filled skutterudites CeFe_{4-x}Zn_xSb₁₂." *J. Solid State Chem.*, **187**, 316 (2012).
31. H.-S. Kim et al., "Characterization of Lorenz number with seebeck coefficient measurement." *APL Materials*, **3**, 041506 (2015).
32. C. Xu et al., "Thermoelectric properties of skutterudites Co_{4-x}Ni_xSb_{11.9-y}TeySe_{0.1}." *J. Electron. Mater.*, **43**, 2224 (2014).
33. T. Caillat, A. Borshevsky, and J. P. Fleurial, "Properties of single crystalline semiconducting CoSb₃." *J. Appl. Phys.*, **80**, 4442 (1996).